Observation of Rydberg Wave Packet Dynamics in a Coulombic and Magnetic Field

J. Wals,[1] H. H. Fielding,[1] J. F. Christian,[2] L. C. Snoek,[2] W. J. van der Zande,[2] and H. B. van Linden van den Heuvell[1,2]

[1]*van der Waals-Zeeman Laboratory, University of Amsterdam, Valckenierstraat 65, 1018 XE Amsterdam, The Netherlands*

[2]*FOM-Institute for Atomic and Molecular Physics, Kruislaan 407, 1098 SJ, Amsterdam, The Netherlands*

(Received 17 January 1994)

Rydberg electron wave packets are investigated, using phase-modulated detection. In the absence of any external field we observe pure radial motion of a bound electron wave packet showing both the first integer revival and all fractional revivals up to the seventh order; in the presence of a magnetic field (0.81 T) both paramagnetic and diamagnetic effects are observed. Paramagnetism is visible in the time-correlation function of the wave packet as a sinusoidal intensity modulation, with a period of 43 ps, superimposed on the radial motion; the diamagnetism is observed as a decrease in the radial recurrence times (by up to 35%).

PACS numbers: 42.50.Md, 32.60.+i, 32.80.Rm

One of the most important reasons for studying the real-time wave packet dynamics of electrons in Rydberg atoms is to establish the limits of the link with the classical dynamics of the system following from the correspondence principle; this is particularly interesting in the case of electron motion in a combined Coulombic and magnetic field, where the classical system becomes chaotic in the limit of a strong magnetic field and a small binding energy [1–3]. At first sight it is surprising that time-resolved spectroscopy, so successful for many aspects of electron dynamics in Rydberg atoms, is not yet employed successfully for the problem of an electron in a combined magnetic and Coulombic field. In general, when a wave packet undergoes dispersion or fragmentation the resulting signals are small and therefore require a high detection efficiency. For these reasons, we combine an experimental study of Rydberg electron wave packets in Coulombic and magnetic potentials with the phase-modulated detection technique proposed by Noordam *et al.* [4] and implemented experimentally and described in detail by Broers *et al.* [5] and Christian *et al.* [6]; in this novel detection scheme, the monitored electron signal is proportional to the overlap of the wave function after delay τ and the original wave function at $t = 0$, i.e., the time-correlation function $|\langle\psi(0)|\psi(\tau)\rangle|$. The work we present here extends the original scheme to an electric field-free situation using a pulsed electric field and makes the real-time dynamics of a Rydberg electron wave packet in a combined Coulombic and magnetic potential accessible for experiments.

Rydberg states of rubidium are excited coherently from the $5s$ ground state using the frequency-doubled light of a synchronously pumped, cavity-dumped, tunable dye laser (3.8 MHz, 5 mW, 297 nm, 2.1 ps, bandwidth $\sim$7 cm^{-1}). A Michelson interferometer is used to split the laser pulse into two identical pulses. A precision translation stage in one arm of the interferometer is used to delay one pulse with respect to the other. The phase difference, i.e., the *precise* delay, between the two pulses is modulated at 6 kHz by wiggling a quartz plate in the "fixed-delay" arm of the Michelson interferometer. The polarization of the light is set by means of a Soleil-Babinet compensator to be either parallel or perpendicular to the magnetic field axis, and the light is focused with an $f = 25$ cm quartz lens into the source region of a magnetic-bottle electron spectrometer. The excitation of the rubidium atoms takes place in a magnetic field which can be varied over the range 0–0.81 T, between two tantalum plates (15 mm diameter with 2.5 mm diameter holes covered by coarse tungsten mesh) separated by 3.9 mm; the excited Rydberg atoms are subsequently field ionized with a pulsed electric field of 295 V/cm (3.8 MHz), which was generated by using a fast power amplifier and an oscillating circuit that was tuned into resonance with the repetition frequency of the laser. We estimate that the coherent excitation takes place in stray fields of no more than $\sim$0.5 V/cm. The lowest Rydberg level that could be ionized in this way has an effective principal quantum number $n \approx 33$. The two laser pulses create two identical wave packets that, at the moment of their creation, are located in the core region. It depends on both the radial position and the angular momentum of the first wave packet whether or not, at the moment of creation of the second wave packet, there will be interference between the two wave packets. If there is interference, it will oscillate between being destructive and constructive with the same frequency as the modulation of the phase delay between the two optical pulses which excited the wave packets (in this particular experiment 6 kHz). The total population of the Rydberg states, remaining after the two pulses, is field ionized and as a consequence, the resulting signal after passing through a bandpass filter that filters the 6 kHz component of the total signal, is a measure of the interference between the two wave packets.

The first results we report were made in the absence of any external electric or magnetic field. Because of the single-photon absorption selection rules, we excite

0031-9007/94/72(24)/3783(4)$06.00

coherently a number of Rydberg p states lying within the bandwidth of the exciting laser pulse; in this way, a superposition is formed over a range of principal quantum numbers n (with energies E_n) with an average value $\bar{n}$, creating a nonstationary wave function

$$\Psi(\mathbf{r},t)=\sum_n a_n e^{iE_n t}R_{nl}(r) \quad . \tag{1}$$

$R_{nl}(r)$ is the hydrogen radial wave function and a_n is given by the Gaussian envelope of the exciting laser pulse. The resultant wave packet is localized in the radial coordinate and oscillates at the classical orbit period $t_{\rm cl}=2\pi\bar{n}^3$. The long time behavior is especially interesting and has been studied experimentally [7,8] and theoretically [9–13]; however, with our improved detection scheme we are able to resolve previously unobserved features. In Fig. 1(a) we present a measurement of the radial recurrences for excitation of Rydberg levels centered around $E=-50.7$ cm^{-1} ($\bar{n}=46.5$, $\Delta n\approx 6.5$, where Δn is the number of states involved in the superposition, and is determined by taking one laser bandwidth either side of the central frequency). Classically, the peaks in the recurrence spectrum represent the return of the electron to the core region. Gradually, the wave packet disperses due to the fact that the energy levels of the contributing Rydberg states are not equidistant, until eventually, after approximately 237 ps, they rephase and the original classical picture once again becomes apparent [8,14]. The period of this decay and revival is given by $T_{\rm rev}=\frac{\bar{n}}{3}t_{\rm cl}$ [10]. The spreading of the wave packet is smooth until the moment that the wave packet is distributed completely over the orbit. At this moment the head of the wave packet meets its tail, interference occurs, and as a result a number of small wave packets appear. In the recurrence spectrum this interference manifests itself as peaks with higher periodicity, the so-called fractional revivals [11,13]. Expanding the energy E_n in the phase factor in Eq. (1) around the average energy of the wave packet $E_{\bar{n}}$ gives nonlinear terms responsible for the interference effects. The second order nonlinear phase reflects the nonequidistance of the stationary eigenstates in the superposition and results in the full revival at $T_{\rm rev}$ and all the fractional revivals for $\tau<T_{\rm rev}$. The contribution of this term becomes important after $\tau=\frac{8\bar{n}}{3\Delta n}t_{\rm cl}$ (Δn defined as above), in our case $2.9t_{\rm cl}$ and $1.5t_{\rm cl}$ for Fig. 1 and the inset, respectively. In the case that $\Delta n/\bar{n}$ is small and the third-order nonlinear phase is negligible, the peaks in the interference pattern at $T_{\rm rev}$ will be shifted $t_{\rm cl}/2$, i.e., the revival takes place at the outer turning point [8,13]. The third order term starts to be important after $\tau=\frac{4\bar{n}^2}{\Delta n^3}$ and has the effect of shifting the peaks in the interference pattern. When this term is no longer negligible, the peaks in the revivals will no longer be shifted according to the second order term, but will have a shift depending on the size of the ratio $\Delta n/\bar{n}$. As a result, the overall intensity profile of the recurrence spectrum is determined by $\bar{n}$, that gives both $t_{\rm cl}$ and $T_{\rm rev}$, while the precise structure of the interference pattern depends on the ratio $\Delta n/\bar{n}$ and the exact level structure of the superposition. Since the quantum defect changes the structure of the energy levels in the superposition without changing the average energy or the number of levels, it has a similar effect on the interference pattern as the third order nonlinear phase. The peaks are shifted towards shorter delay by an amount proportional to the quantum defect in modulo 1. From the recurrence spectrum in Fig. 1(a) the measured quantum defect is 0.62 ± 0.03 (mod 1) and is in good agreement with the known value (0.65 mod 1). Figure 1(b) shows the calculated transition probability, $|\langle\psi_{1s}|r|\Psi(\mathbf{r},t)\rangle|^2$, for rubidium adopting the rotating wave approximation and assuming a Gaussian pulse with a FWHM bandwidth of 7 cm^{-1}. Hydrogenic wave functions are used and the quantum defect for rubidium was incorporated in the phases of the stationary states. There is a rapid decay of the envelope of the signal with increasing delay in the experimental recurrence spectra. This is not related to the evolution of the wave packet in the time interval between the two pulses, but can be attributed partly to a coherence loss as atoms move par-

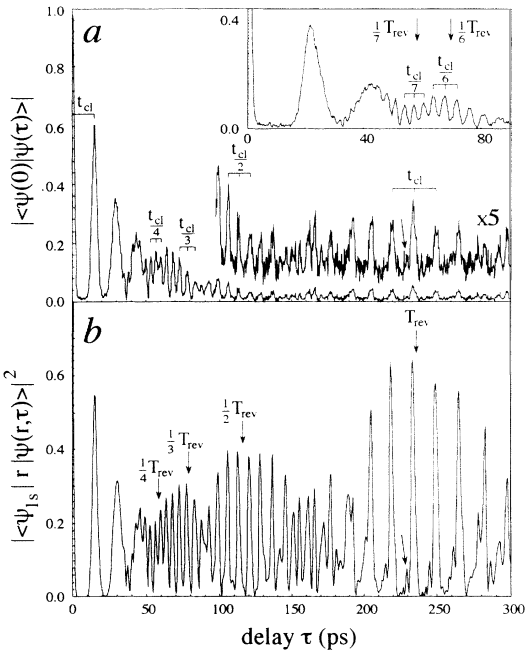

FIG. 1. []Field-free recurrence spectra for excitation of a Rydberg electron wave packet around $E=-50.7$ cm^{-1} ($\bar{n}=46.5, \Delta n\approx 6.5$). (a) Measured spectrum in rubidium. (b) Calculated time-dependent transition probability spectrum for rubidium. Clearly visible is the first integer revival around $\tau=237$ ps. Fractional revivals of order 2, 3, and 4 are visible at $T_{\rm rev}/2$, $T_{\rm rev}/3$, and $T_{\rm rev}/4$, respectively, where $T_{\rm rev}=\frac{\bar{n}}{3}t_{\rm cl}$; $t_{\rm cl}$ is the classical orbit period $2\pi\bar{n}^3$. The inset shows fractional revivals with period $t_{\rm cl}/6$ at $T_{\rm rev}/6$ and $t_{\rm cl}/7$ at $T_{\rm rev}/7$ for excitation energy $E=-38.6$ cm^{-1} ($\bar{n}=53.3, \Delta n\approx 9.9$). The small wave packet preceding the main wave packet in the integer revival resulting from the third-order nonlinear phase is indicated with an arrow.

allel to the laser beam over a distance comparable with a quarter of the laser wavelength; in addition, any distortion of the wave front of the laser beam results in a poorer overlap of the two pulses in the focus in the interaction region with increasing delay between the pulses.

Introducing a magnetic field reduces the original spherical symmetry of the system to one with cylindrical symmetry around the magnetic field axis; the azimuthal quantum number m_l and parity are still conserved but l is no longer a good quantum number. The resulting Hamiltonian is not separable and has, consequently, no analytic solution. In the combined magnetic field and Coulombic potential, the Hamiltonian becomes (in a.u.):

$$\mathcal{H} = \mathcal{H}_0 + \tfrac{1}{2} m_l B + \tfrac{1}{8} B^2 (x^2 + y^2) \quad , \tag{2}$$

where $\mathcal{H}_0$ is the zero-field Hamiltonian and the magnetic field axis is directed in the z direction; B is in units of $B_c = 2.35 \times 10^5$ T. The second term in Eq. (2) gives the paramagnetic (i.e., the linear Zeeman) contribution, which is independent of n and in fact of any atomic structure. The last term in Eq. (2) gives the diamagnetic contribution which is proportional to n^4. In Fig. 2 time-resolved recurrence spectra are presented for both parallel (exciting $m_l = 0$ levels) and perpendicular (exciting $|m_l| = 1$ levels) laser polarization in a magnetic field of 0.81 T and excitation energy $E = -87.0$ cm^{-1} ($\bar{n} = 35.5$). With perpendicular (σ) polarization we observe a sinusoidal intensity modulation with a period of approximately 43 ps corresponding to an energy spacing of ~ 0.8 cm^{-1}, which is superimposed on the radial motion. For parallel (π) polarization no such modulation is observed. These observations are in agreement with elementary considerations based on the Zeeman effect. The sinusoidal modulation arises from the superposition of $|m_l| = 1$ wave functions ($\Delta E = 0.76$ cm^{-1}) and can be pictured as a rotation of the electron charge density around the magnetic field axis with the Larmor frequency, given by $\omega_L = B/2$, resulting in a rotation period of 88 ps. The first and the second wave packet interfere and therefore contribute to the detected, modulated signal when their wave functions are not perpendicular. The result of the projection of the circular motion of the wave function onto the plane of the laser polarization is a sinusoidal modulation with a period of 44 ps. For $m_l = 0$ there is no rotation of the wave function and consequently no such intensity modulation of the radial motion is observed with parallel polarization.

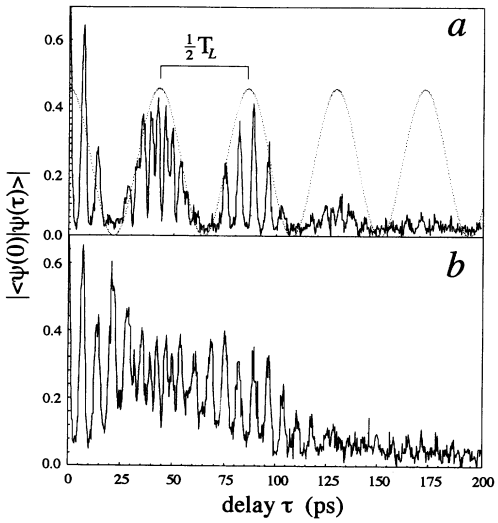

FIG. 2. Recurrence spectra for both (a) σ and (b) π laser polarization in the presence of a magnetic field for excitation around $E = -87.0$ cm^{-1} ($\bar{n} = 35.5$). The modulation with a period of 43 ps in (a) is attributed to the rotation of the wave function around the magnetic field axis. There is no rotation, and hence no modulation for $m_l = 0$ (b). T_L is the Larmor period.

Increasing the photon energy, i.e., increasing $\bar{n}$, results in an increase of the classical Kepler orbit period. In Fig. 3, the first radial recurrence times are plotted both for the field-free regime and the regime where a magnetic field is present. Applying a magnetic field has the effect of reducing the recurrence times; this effect is larger for σ polarization than for π polarization. In order to confirm our interpretation that the decrease in recurrence times with increasing excitation energy can be attributed to the diamagnetic contribution, we have performed a matrix diagonalization calculation to simulate the corresponding frequency spectrum. The Hamiltonian given above, Eq. (2), was diagonalized in a hydrogenic basis set, in the region from -90 to -60 cm^{-1}, including $n = 33$ to $n = 60$. The well known matrix elements are [15]

$$\frac{B^2}{8} \frac{2(l^2 + l - 1 + m^2)}{(2l-1)(2l+3)} \sigma(nl; n'l') \quad \text{if} \quad l' = l, \tag{3a}$$

$$\frac{-B^2}{8} \left(\frac{(l+m+2)(l+m+1)(l-m+2)(l-m+1)}{(2l+5)(2l+3)^2(2l+1)} \right)^{\frac{1}{2}} \times \sigma(nl; n'l') \quad \text{if} \quad l' = l+2 \quad , \tag{3b}$$

where

$$\sigma(nl; n'l') = \int_0^\infty r^2 R(nl) R(n'l') dr \quad . \tag{3c}$$

$\sigma(nl; n'l')$ represents the overlap integral and was integrated numerically [16], incorporating the quantum defects for rubidium. The calculated frequency spectrum of rubidium contains isolated p levels with respect to the high-l manifolds; thus, distribution of the p character over the manifold begins at higher magnetic fields, or equivalently for a fixed B field at a higher $\bar{n}$, than in hydrogen. This l mixing is complete when n mixing begins to occur and in analogy with the electric field case, the lowest magnetic field for which this n mixing occurs could be named the Inglis-Teller limit. Using the results of the diagonalization calculation we deduce radial recurrence times for rubidium in a magnetic field which are in good agreement with the measured recurrence times (Fig.

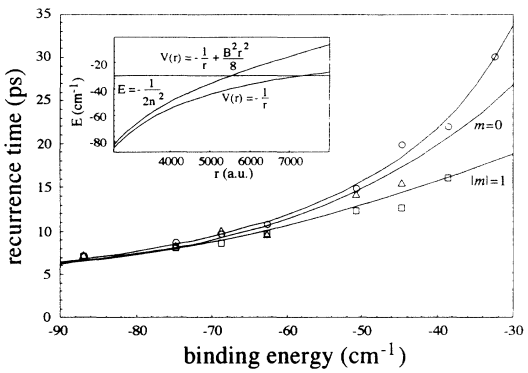

FIG. 3. []Radial recurrence times plotted for both the field-free case (circles) and the magnetic field case and also for both parallel (triangles) and perpendicular (squares) laser polarization. The theoretical curves represent the diagonalization calculation for Rb in a magnetic field of 0.81 T. The uppermost curve shows the field-free recurrence times $t_{cl} = 2\pi\bar{n}^3$. The inset shows the effect of the magnetic field on the position of the outer turning points in the plane perpendicular to the B-field axis. Potential curves both with and without the magnetic field present are given, as well as the energy of $n = 60$ (horizontal line).

3). The smaller radial period in the magnetic field can be explained using a classical picture: In the plane perpendicular to the magnetic field the well of the Coulombic potential is narrowed and the outer turning point is changed to $2n^2 - \frac{5}{4}n^8B^2 + \mathcal{O}(B^3)$; for $n = 60$, the outer turning point is brought closer to the core by approximately 35%. The inset in Fig. 3 shows the pure Coulombic potential as well as the Coulombic potential perturbed by the diamagnetic interaction. The horizontal line represents the energy corresponding to $n = 60$ and the crossings with this energy determine the outer turning points in both potentials. An electron excited by σ-polarized light travels along an orbit which lies predominantly in the plane perpendicular to the magnetic field, while one excited by π polarized light travels predominantly along the magnetic field axis. Therefore, the largest reduction in recurrence time is expected for an electron excited by σ polarization.

In conclusion, we have investigated the real-time dynamics of Rydberg electron wave packets in rubidium, using a phase-modulated detection technique and we observed the dynamics of a radial wave packet in detail as well as the effects of both paramagnetism and diamagnetism. In the absence of any external field we have observed for the first time all fractional revivals of a Rydberg electron wave packet up to the seventh order. For a laser polarization perpendicular to the magnetic field the observed sinusoidal intensity modulation has been attributed to the $|m_l| = 1$ splitting of the energy levels in a magnetic field and is viewed as a rotation of the wave function around the magnetic field axis with the Larmor frequency. It has been shown experimentally that the quadratic energy shift in a magnetic field decreases the radial recurrence times, which we attribute to a decrease in the outer turning point of the classical electron orbit.

J.W. and H.H.F. like to acknowledge the hospitality of the FOM Institute for Atomic and Molecular Physics. L.D. Noordam, B. Broers, and A.N. Buijserd are acknowledged for their work on the phase-modulated detection technique. The work in this paper is part of the research program of the "Stichting voor Fundamenteel Onderzoek van de Materie" (Foundation for Fundamental Research on Matter) and was made possible by financial support from the "Nederlandse Organisatie voor Wetenschappelijk Onderzoek" (Netherlands Organization for the Advancement of Research). H.H.F. is a Research Fellow of the Royal Commission for the Exhibition of 1851 (U.K.).

[1] G. Alber, Z. Phys. D **14**, 307 (1989).
[2] M.L. Du and J.B. Delos, Phys. Rev. A **38**, 1896 (1988).
[3] J.A. Yeazell, G. Raithel, L. Marmet, H. Held, and H. Walther, Phys. Rev. Lett. **70**, 2884 (1993).
[4] L.D. Noordam, D.I. Duncan, and T.F. Gallagher, Phys. Rev. A **45**, 4734 (1992).
[5] B. Broers, J.F. Christian, J.H. Hoogeraad, W.J. van der Zande, H.B. van Linden van den Heuvell, and L.D. Noordam, Phys. Rev. Lett. **71**, 344 (1993).
[6] J.F. Christian, B. Broers, J.H. Hoogenraad, W.J. van der Zande, and L.D. Noordam, Opt. Commun. **103**, 79 (1993).
[7] A. ten Wolde, L.D. Noordam, A. Lagendijk, and H.B. van Linden van den Heuvell, Phys. Rev. Lett. **61**, 2099 (1988).
[8] J.A. Yeazell, M. Mallalieu, and C.R. Stroud, Jr., Phys. Rev. Lett. **64**, 2007 (1990).
[9] G. Alber, H. Ritsch, and P. Zoller, Phys. Rev. A **34**, 1058 (1986).
[10] J. Parker and C.R. Stroud, Jr., Phys. Rev. Lett. **56**, 716 (1986).
[11] Z. Dačić Gaeta and C.R. Stroud, Jr., Phys. Rev. A **42**, 6308 (1990).
[12] S.D. Boris, S. Brandt, H.D. Dahmen, T. Stroh, and M.L. Larsen, Phys. Rev. A **48**, 2574 (1993).
[13] I. Sh. Averbukh and N.F. Perelman, Phys. Lett. A **139**, 449 (1989).
[14] D.R. Meacher, P.E. Meyler, I.G. Hughes, and P. Ewart, J. Phys. B **24**, L63 (1991).
[15] R.H. Garstang, Rep. Prog. Phys. **40**, 105 (1977).
[16] M.L. Zimmerman, M.G. Littman, M.M. Kash, and D. Kleppner, Phys. Rev. A **20**, 2251 (1979).